Inorganic Chemistry

Article

pubs.acs.org/IC

Highly Selective Recognition and Fluorescence Imaging of Adenosine Polyphosphates in Aqueous Solution

Mei Zhang, Wen-Juan Ma, Chun-Ting He, Long Jiang, and Tong-Bu Lu*

MOE Key Laboratory of Bioinorganic and Synthetic Chemistry, State Key Laboratory of Optoelectronic Materials and Technologies, School of Chemistry and Chemical Engineering, Sun Yat-Sen University, Guangzhou 510275, People's Republic of China

Supporting Information

ABSTRACT: The design and synthesis of chemosensors for the recognition of a certain nucleoside polyphosphate among various structurally similar nucleoside polyphosphates remain a fundamental challenge. Herein, we report the new fluorescent chemosensor $[Zn_2L](ClO_4)_4$ (**1**; L = (3,6,10,13,17,20,24,27-octaaza-1,15(2,6)-dipyridina-8,22(9,10)-dianthracenacyclooctacosaphane), which can selectively recognize adenosine polyphosphates (ATP and ADP) among various nucleoside polyphosphates, with a large fluorescence enhancement (F_{max}/F_0 = 70 and 80 for ATP and ADP, respectively) and strong binding affinity ($K = 3.1 \times 10^{11}$ M^{-1} for $[Zn_2HL(H_{-1}ATP)_2]^-$, 2.8×10^{11} M^{-1} for $[Zn_2L(H_{-1}ATP)_2]^{2-}$, and 1.5×10^{13} M^{-1} for $[Zn_2L(H_{-1}ADP)_2]^{2-}$) in aqueous solution at physiological pH 7.40. The structure of $[Zn_2L](P_2O_7)$ (**2**) was investigated, which shows that μ_2-pyrophosphate anions alternately link $[Zn_2L]^{4+}$ cations to generate a 1D coordination polymer. The results of ^{31}P NMR studies and DFT calculations reveal that the two Zn(II) ions in **1** can interact with ATP/ADP anions through coordination interactions between Zn(II) and the polyphosphate groups, and two anthracene moieties in **1** can interact with adenine groups from two ATP or ADP anions through stacking interactions to form a sandwichlike structure. These multiple recognition interactions between **1** and ATP/ADP enhance the affinity and selectivity of **1** toward ATP/ADP. Due to its highly selective and sensitive ability to detect adenosine polyphosphates, **1** was successfully applied to fluorescence imaging for ATP and ADP in living cells, demonstrating the potential utility of **1** as a fluorescent chemosensor for detecting ATP and ADP.

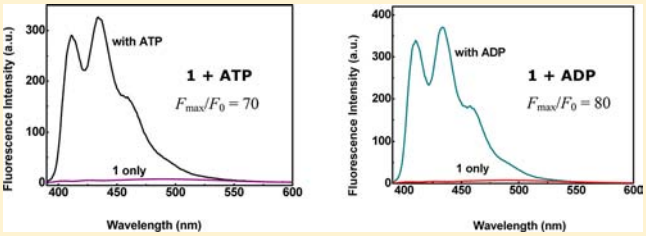

INTRODUCTION

Phosphate recognition continues to attract much attention, as phosphates play a fundamental role in many biological processes.[1] Adenosine-5′-triphosphate (ATP) is well-known as an universal energy currency in all biological systems; thus, it is a significant target to be conventionally monitored.[2] Given the biological importance of phosphate anion species, continuous efforts have been made to design and synthesize chemosensors for the recognition of phosphates.[3−8] Micheloni and co-workers found that dinuclear polyamino-phenolic Zn(II) complexes are able to discriminate phosphate (Pi) and pyrophosphate (PPi) in water.[6c] Churchill and co-workers reported a chiral fluorescent zinc complex for the fluorometric and colorimetric sensing of PPi, ATP, and ADP in water at physiological pH.[6d] Hamachi and co-workers have extensively pursued Zn(II)−dipicolylamine (dpa) complexes as chemosensors for the detection of phosphates and nucleoside polyphosphates.[7] Though the reported chemosensors show selective recognition of phosphates, most of them lack selectivity for a certain nucleoside polyphosphate, as they only contain the recognition sites for phosphate groups, and only a few reported chemosensors display selective recognition toward a certain nucleoside polyphosphate.[8] Recently, Ahn and co-workers reported a mononuclear Zn−pyridine complex[9] that can interact with an individual ATP/ADP through the coordination interaction of Zn(II) with the terminal phosphate groups of ATP/ADP, as well as the $\pi\cdots\pi$ interaction between the fluorophore of the ligand and the nucleobase of ATP/ADP, and the complex displays recognition of ATP and ADP over AMP and other anions. However, this Zn−pyridine complex lacks the selectivity for ATP and ADP from structurally similar nucleoside polyphosphates such as GTP, CTP, and TTP. It is still a challenging task to discriminate a certain nucleoside polyphosphate among various structurally similar nucleoside polyphosphates such as ATP, GTP, UTP, TTP, and CTP,[8a] especially for a chemosensor with a strong binding affinity toward a given nucleoside polyphosphate and a large enhancement of fluorescence upon the addition of nucleoside polyphosphate.

Herein, we report such a chemosensor of $[Zn_2L](ClO_4)_4$ (**1**; L = (3,6,10,13,17,20,24,27-octaaza-1,15(2,6)-dipyridina-8,22-(9,10)-dianthracenacyclooctacosaphane), which displays a highly selective recognition of adenosine polyphosphates (ATP and ADP) over other structurally similar nucleoside polyphosphates (Scheme 1). Most importantly, a very large enhancement of the fluorescence of **1** is observed upon addition of ATP and ADP, with F_{max}/F_0 = 70 and 80 for ATP

Received: November 7, 2012
Published: April 5, 2013

   dx.doi.org/10.1021/ic302435g | Inorg. Chem. 2013, 52, 4873−4879

Scheme 1. Strategy for the Synthesis of 1

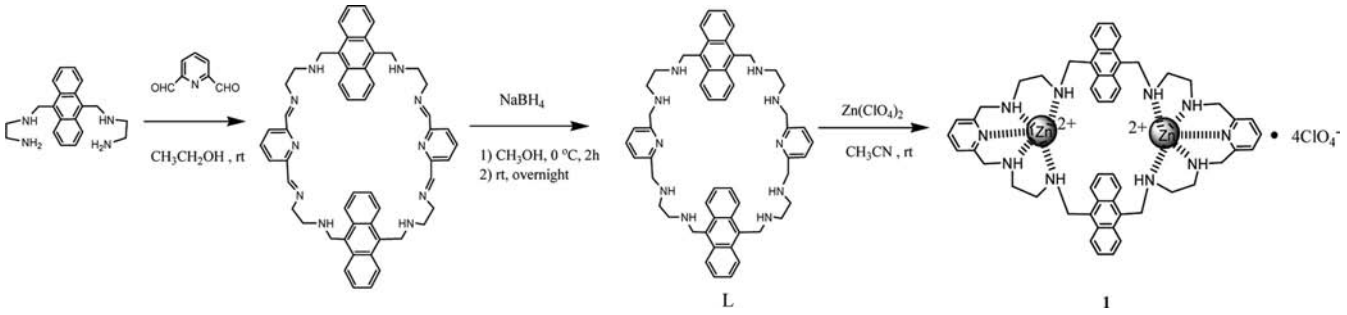

and ADP, respectively. The possible binding mode of **1** with ATP (and ADP) was given on the basis of experimental results and DFT calculations.

EXPERIMENTAL SECTION

General Information and Materials. Unless otherwise noted, materials were obtained from commercial suppliers and were used without further purification. ^{1}H and ^{13}C NMR spectra were recorded using a Varian Mercury 300 spectrometer, and ^{31}P NMR spectra were recorded using a Bruker Advance AV 400 spectrometer. Chemical shifts were expressed in ppm. Mass spectra were obtained using a Thermo Finnigan LCQ DECA XP ion trap mass spectrometer. Elemental analyses were determined using an Elementar Vario EL elemental analyzer. Thermogravimetric (TG) analysis data were collected on a Netzsch TG-209 instrument under a nitrogen atmosphere in the temperature range 20−800 °C, with a heating rate of 10 °C min^{-1}. Microscopic observations were assessed by a laser scanning confocal microscope (Zeiss LSM710). 9,10-Bis[*N*-(aminoalkylene)aminomethyl]anthracene[10] and 2,6-pyridinedicarboxaldehyde[11] were synthesized following the published procedures.

Synthesis of L. A solution of 2,6-pyridinedicarboxaldehyde (1.35 g, 10.0 mmol) in ethanol (80 mL) was slowly added to an ethanol solution (500 mL) of 9,10-bis[*N*-(aminoalkylene)aminomethyl]-anthracene (3.22 g, 10.0 mmol). The mixture was stirred in the dark for 12 h, and the resulting yellow powder (3.2 g, 76%) was separated from the solution by vacuum filtration and washed with ethanol. Then $NaBH_4$ (1.89 g, 50 mmol) was added in small portions to a magnetically stirred solution of the yellow powder (2.1 g, 2.5 mmol) in MeOH (150 mL). The mixture was stirred at 0 °C for 2 h and then stirred at room temperature overnight in the dark. The obtained solution was evaporated under vacuum to almost dryness, and H_2O (200 mL) was added. The aqueous solution was extracted with CH_2Cl_2 (200 mL × 5), and the combined organic solution was dried over $MgSO_4$. The solvent was removed under reduced pressure, and the residue was recrystallized in methanol to afford pure ligand L as a yellow solid in 46% yield (0.978 g). ^{1}H NMR ($CDCl_3$, 300 MHz): δ 8.27 (dd, ^{4}J = 3.21 and ^{3}J = 6.82 Hz, 8H), 7.48 (d, ^{3}J = 7.58 Hz, 2H), 7.42 (dd, ^{4}J = 3.13 and ^{3}J = 6.93 Hz, 8H), 7.01 (d, ^{3}J = 7.61 Hz, 4H), 4.52 (s, 8H), 3.74 (s, 8H), 2.85 (t, ^{3}J = 5.51 Hz, 8H), 2.66 (t, ^{3}J = 5.53 Hz, 8H). ^{13}C NMR ($CDCl_3$, 75 MHz): δ 159.23, 136.82, 132.23, 130.22, 125.70, 125.14, 120.47, 77.41, 55.08, 50.03, 49.08, 46.17. ESI-MS: m/z 851 $[L + H]^+$. Anal. Calcd for $C_{54}H_{62}N_{10}\cdot1.5H_2O$ ($L\cdot1.5H_2O$): C, 73.86; H, 7.46; N, 15.95. Found: C, 73.88; H, 7.50; N, 15.83.

Synthesis of $[Zn_2L](ClO_4)_4$ (1). An acetonitrile solution (8 mL) of $Zn(ClO_4)_2\cdot6H_2O$ (0.018 g, 50 μmol) was added dropwise to a solution of L (0.021 g, 25 μmol) in acetonitrile (10 mL), and the mixture was stirred at room temperature for 2 h. Upon slow evaporation of the resulting solution, yellow crystals of $\mathbf{1}\cdot1.5H_2O\cdot2CH_3CN$ were obtained. Yield: 0.0136 g, 35%. ESI-MS for $C_{54}H_{62}N_{10}\cdot2Zn\cdot3ClO_4$: m/z 1279 $[\mathbf{1} - ClO_4^-]^+$. Anal. Calcd for $C_{54}H_{62}N_{10}\cdot2Zn\cdot4ClO_4\cdot1.5H_2O$ ($\mathbf{1}\cdot1.5H_2O$): C, 46.10; H, 4.66; N, 9.96. Found: C, 45.87; H, 4.88; N, 9.80.

Caution! Perchlorate salts of metal complexes with organic ligands are potentially explosive. They should be handled with care and prepared only in small quantities.[12]

Synthesis of $[Zn_2L]P_2O_7$ (2). A solution of $Na_4P_2O_7\cdot10H_2O$ (0.009 g, 0.02 mmol) in water (4 mL) was slowly diffused with an acetonitrile solution (4 mL) of **1** (0.014 g, 0.01 mmol) in a tube. Four days later, bright yellow crystals formed at the water/acetonitrile interface, which were dried under vacuum for 15 h. Yield: 2.0 mg, 22%. Anal. Calcd for $C_{54}H_{62}N_{10}O_7P_2Zn_2\cdot8H_2O$ ($\mathbf{2}\cdot8H_2O$): C, 49.89; H, 6.05; N, 10.77. Found: C, 50.02; H, 6.39; N, 10.69.

Fluorescence Titration Experiments. Fluorescence spectra were recorded on a Shimadzu RF-5301PC spectrofluorophotometer. Fluorescence titration experiments of **1** with ATP and ADP were performed in aqueous solution (HEPES buffer, pH 7.40) at 25 °C. The fluorescence quantum yields of the adducts of **1** with ATP and ADP were calculated under neutral aqueous conditions (40 mM HEPES, pH 7.4), by using quinine sulfate (Φ_F = 0.54 in 0.05 M H_2SO_4) as a standard. The fluorescence quantum yields were calculated using the equation[13] $\Phi_u = \Phi_s A_s F_u(n_u)^2/(A_u F_s(n_s)^2)$, where A_s and A_u are the standard and unknown compound absorbances, respectively, F_s and F_u are the areas of fluorescent peaks of the standard and unknown compound, respectively, n_s and n_u are the refractive indices of the solvents used for the standard and unknown compound, respectively, and Φ_s and Φ_u are the fluorescent quantum yields of the standard and unknown compound.

Potentiometric Measurements. The potentiometric titrations were carried out at 298.1 ± 0.1 K in 0.1 M NaCl with a Metrohm 702GPD Titrino, equipped with a combined Metrohm electrode which was calibrated according to the Gran method.[14] The electrode system was calibrated with buffers and checked by titration of HCl with NaOH solution (0.10 M). All titrations were carried out in aqueous solutions under nitrogen and initiated by adding fixed volumes of 0.10 M standard NaOH in small increments to the titrated solution. Triplicate measurements were performed, for which the experimental error was below 1%. The titration data were fitted from the raw data with the Hyperquad 2000 program[15] to calculate the equilibrium constants.

Cell Culture. HeLa cells were cultured in Dulbecco's Modified Eagle's Serum (DMEM; Invitrogen) with 10% fetal bovine serum (FBS; Invitrogen). One day before imaging, the cells were plated on glass-bottomed dishes (MatTek). For imaging, one group of cells was treated with apyrase in PBS (pH 6.13) for 70 min, and another group was not treated. Then two groups of cells were exposed to 100 μM of **1** for 15 min at 37 °C under 5% CO_2 and washed with PBS buffer solution (pH 7.40) three times. Microscopic observation was performed with a laser scanning confocal microscope (Zeiss LSM710). Images were recorded with a excitation wavelength of 405 nm by using a 40× oil immersion objective lens.

X-ray Crystallography. Single-crystal X-ray diffraction data for $\mathbf{1}\cdot1.5H_2O\cdot2CH_3CN$ and $\mathbf{2}\cdot19H_2O$ were collected at 150 K on an Agilent Technologies Gemini A Ultra system, with Cu Kα radiation (λ = 1.54178 Å). The empirical absorption corrections were applied using spherical harmonics, implemented in the SCALE3 ABSPACK scaling algorithm. The structures were solved using direct methods and refined by the full-matrix least-squares method on F^2, which yielded

dx.doi.org/10.1021/ic302435g | Inorg. Chem. 2013, 52, 4873−4879

the positions of all non-hydrogen atoms. These were refined first isotropically and then anisotropically. All of the hydrogen atoms of the ligands were placed in calculated positions with fixed isotropic thermal parameters and included in the structure factor calculations in the final stage of full-matrix least-squares refinement. The water molecules in **2**·19H_2O were refined isotropically, and hydrogen atoms of water molecules were not added due to a great number of disordered water molecules. All calculations were performed using the SHELXTL system of computer programs.[16] The details of crystallographic data for **1**·1.5H_2O·2CH_3CN and **2**·19H_2O are summarized in Table 1.

Table 1. Crystal Data and Structure Refinement Details for 1·1.5H_2O·2CH_3CN and 2·19H_2O

	1·1.5H_2O·2CH_3CN	**2**·19H_2O
formula	$C_{58}H_{71}N_{12}O_{17.5}Cl_4Zn_2$	$C_{54}H_{100}N_{10}O_{26}P_2Zn_2$
fw	1488.85	1498.15
cryst syst	triclinic	triclinic
T (K)	150(2)	150(2)
space group	$P\bar{1}$	$P\bar{1}$
a/Å	12.5628(5)	10.6866(4)
b/Å	17.2112(9)	17.8276(9)
c/Å	17.4593(7)	19.8301(8)
α/deg	60.847(5)	67.193(4)
β/deg	76.857(4)	81.538(3)
γ/deg	71.887(4)	82.204(4)
V/Å^3, Z	3120.3(2)	3431.8(3)
F(000)	1542	1546
cryst size/mm^3	0.40 × 0.35 × 0.30	0.21 × 0.12 × 0.08
no. of collected/unique rflns (R_{int})	31080/10996 (R_{int} = 0.0361)	20957/11334 (R_{int} = 0.0389)
no. of obsd rflns ($I \geq 2\sigma(I)$)	9699	8874
no. of data/restraints/params	10996/27/995	11334/35/965
D_c/Mg m^{-3}	1.585	1.431
μ/mm^{-1}	3.217	2.033
goodness of fit on F^2	1.027	1.037
R1,[a] wR2[b] ($I \geq 2\sigma(I)$)	0.0394, 0.1012	0.0568, 0.1519
R1, wR2 (all data)	0.0458, 0.1075	0.0739, 0.1673

[a] $R1 = \sum||F_o| - |F_c||/\sum|F_o|$. [b] $wR2 = [\sum[w(F_o^2 - F_c^2)^2]/\sum w(F_o^2)^2]^{1/2}$, where $w = 1/[\sigma^2(F_o)^2 + (aP)^2 + bP]$ and $P = (F_o^2 + 2F_c^2)/3$.

Computational Details. The geometry optimization calculations without any symmetry constraints were carried out using density functional theory (DFT) through the Dmol^3 module of the MS modeling 5.0 package.[17] The widely used generalized gradient approximation (GGA) level of theory with the Perdew–Burke–Ernzerhof (PBE) exchange-correlation energy function was used, together with the double numerical plus polarization (DNP) basis set as well as the effective core potential (ECP) for the metal atoms. In consideration of both the accuracy and calculation efficiency, the convergence criteria were defined as follows: energy, 1.0 × 10^{-5} hartree; maximum force, 2.0 × 10^{-3} hartree Å^{-1}; maximum displacement, 5 × 10^{-3} Å. The Cartesian coordinates for the calculated structures of [$Zn_2L(ADP)_2$] and [$Zn_2L(ATP)_2$] are given in Table S1 and S2 (Supporting Information), respectively.

RESULTS AND DISCUSSION

Crystal Structure of 1·1.5H_2O·2CH_3CN. Single crystals of **1**·1.5H_2O·2CH_3CN were obtained and investigated by X-ray crystallographic analysis. As shown in Figure 1, the ligand L in **1** encapsulates two Zn(II) ions at its two poles. Each Zn(II) ion is five-coordinated with four nitrogen atoms from two ethanediamine moieties and a nitrogen atom from the pyridine group, forming a distorted-trigonal-bipyramidal geometry. The

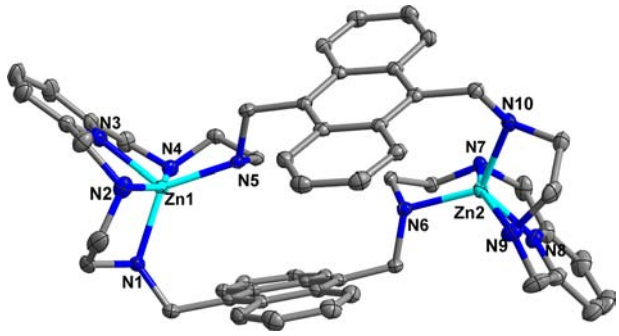

Figure 1. Thermal ellipsoid plot of $[Zn_2L]^{4+}$ with ellipsoids drawn at the 50% probability level.

macrocyclic ligand L is folded to display a chair conformation, in which two anthracene groups in L are not parallel, with the dihedral angle of 22.96° and the shortest centroid–centroid distance of 3.95 Å. The distance between Zn1 and Zn2 is 8.18 Å, indicating the cavity is large enough to encapsulate the guest molecules.

ATP and ADP Recognition. To examine the selectivity of **1** toward nucleoside polyphosphates, the fluorescence changes of **1** with the addition of ATP, ADP, AMP, CTP, GTP, TTP, and UTP were studied. The most striking feature is that the fluorescence intensities of **1** significantly increase upon addition of 2 equiv of ATP and ADP, while the emission intensities do not change or only slightly increase when 2 equiv of AMP, CTP, GTP, TTP and UTP was added (Figure 2a), indicating that **1** can highly recognize ATP and ADP over other nucleoside polyphosphates. The fluorescent quantum yields (Φ_F) of **1** with 2 equiv of ATP and ADP were determined to be 0.07 and 0.12, respectively, which are larger than that of **1** (Φ_F = 0.03). Moreover, the fluorescence intensities of **1** with ATP/ADP in the presence of competing anions of Pi and PPi are almost the same as those of **1** with ATP and ADP (Figure 2a), indicating that the existence of Pi or PPi does not influence the binding and fluorescence emission of **1** with ATP/ADP.

The binding stoichiometries of **1** toward ATP and ADP were investigated by fluorescence titration. The Job plots of **1** with ATP and ADP at 434 nm both display a maximum emission at [ATP]/{[ATP] + $[Zn_2L]^{4+}$} = 0.667 and [ADP]/{[ADP] + $[Zn_2L]^{4+}$} = 0.667, indicating the formation of a 1:2 inclusion compound (see Figure S1, Supporting Information). Figure S2a,b (Supporting Information) shows the fluorescent changes of **1** upon gradual addition of ATP and ADP (0–16 equiv), respectively, giving F_{max}/F_0 values of 70 and 80 for ATP and ADP, respectively (see Figure S3 (Supporting Information); F_{max} is the maximum fluorescence intensity of **1** at 434 nm with the addition of ATP/ADP, and F_0 is the initial fluorescence intensity of **1** at 434 nm without the addition of ATP/ADP). It is worth noting that the maximum fluorescence enhancement reached upon addition of ca. 16 equiv of ATP/ADP instead of 2 equiv of ATP/ADP is probably due to the fact that the reaction is reversible between **1** and ATP/ADP, and not all ATP and ADP forms 2:1 adducts with **1** at 2 equiv of ATP/ADP. A similar phenomenon has also been found in other reported reaction systems of metal complexes with polyphosphates, in which the maximum fluorescence enhancements were reached upon addition of ca. 30 and 40 equiv of PPi, respectively.[18] To our knowledge, a chemosensor displaying such high F_{max}/F_0 values toward ATP and ADP has not been documented so far. Moreover, it is interesting to note that the emission intensities

dx.doi.org/10.1021/ic302435g | Inorg. Chem. 2013, 52, 4873–4879

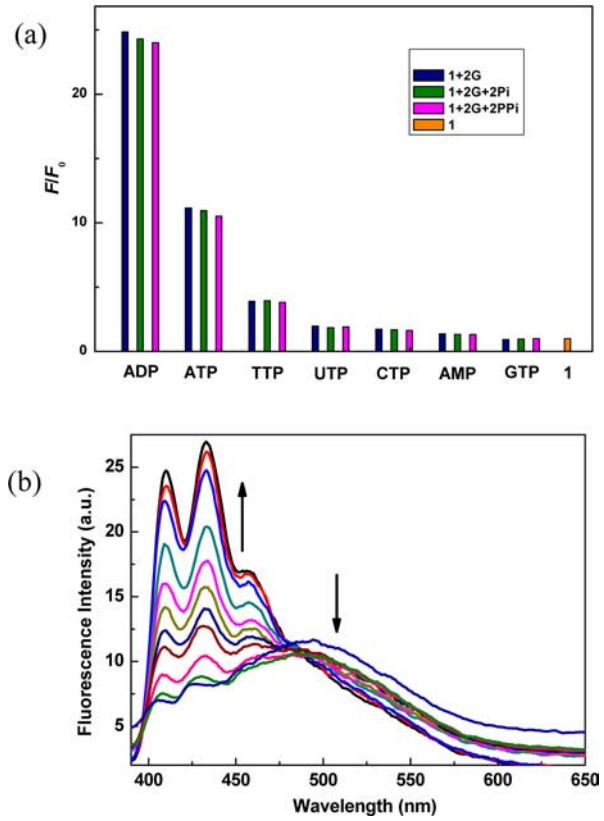

Figure 2. (a) Fluorescence changes of **1** (5 μM) at 434 nm upon the addition of various anions (2 equiv) without and with the existence of Pi and PPi (2 equiv). 2G represents 2 equiv of guests (various anions). (b) Fluorescence changes of **1** (5 μM) with the addition of various amounts of ATP (0–5 μM). Measurement conditions: 40 mM HEPES, pH 7.4, λ_{ex} 368 nm, 25 °C, excitation and emission slit widths 5 and 3 nm, respectively.

of **1** do not change in the presence of other anions such as fluoride, chloride, carbonate, sulfonate, nitrate, acetate, etc. (see Figure S4, Supporting Information), indicating the fluorescence imaging of ATP and ADP in living cells will not be affected by these anions.

ATP, CTP, GTP, TTP, and UTP all contain the same triphosphate groups; thus, the different fluorescence changes between ATP and other nucleotide triphosphates are mainly attributed to the different nucleobases. To investigate the unique role of the adenine in this recognition process, the fluorescence changes of **1** with the addition of ATP (0–1 equiv) were further studied. As shown in Figure 2b, the fluorescence of **1** shows peaks at 409, 434, 457, and 496 nm. The peaks at 409, 434, and 457 nm are attributed to the monomeric emissions of anthracene; the peak at 496 nm comes from the excimer formation of two anthracene groups in L.[19] With the addition of ATP, the excimer peak is gradually quenched, while the intensities of monomeric peaks are enhanced, indicating that the two anthracene moieties can be separated by the adenine group upon addition of ATP, and inserting adenine into two anthracene moieties causes the enhancement of the fluorescence intensity of the anthracene monomer.[8a,b,20] The fluorescence changes upon adding ADP are similar to those found upon adding ATP (Figure S5, Supporting Information).

Potentiometric Studies. Potentiometric titration experiments were carried out to determine the speciation and association constants for the ternary Zn^{2+}–L–ATP and Zn^{2+}–L–ADP systems, and the results are presented in Tables S3 and S4 (Supporting Information). Preliminary potentiometric studies on the coordination ability of L toward Zn^{2+} at variable pH show that the binuclear species prevail in solution over pH 6 for a metal to ligand mole ratio of 2:1 (see Figure S6, Supporting Information), and the species existing to a greater extent are $[Zn_2L]^{4+}$ and $[Zn_2(HL)]^{5+}$ at physiological pH 7.40. The distribution diagrams for the ternary Zn^{2+}–L–ATP and Zn^{2+}–L–ADP systems are presented in Figure 3. For the ATP

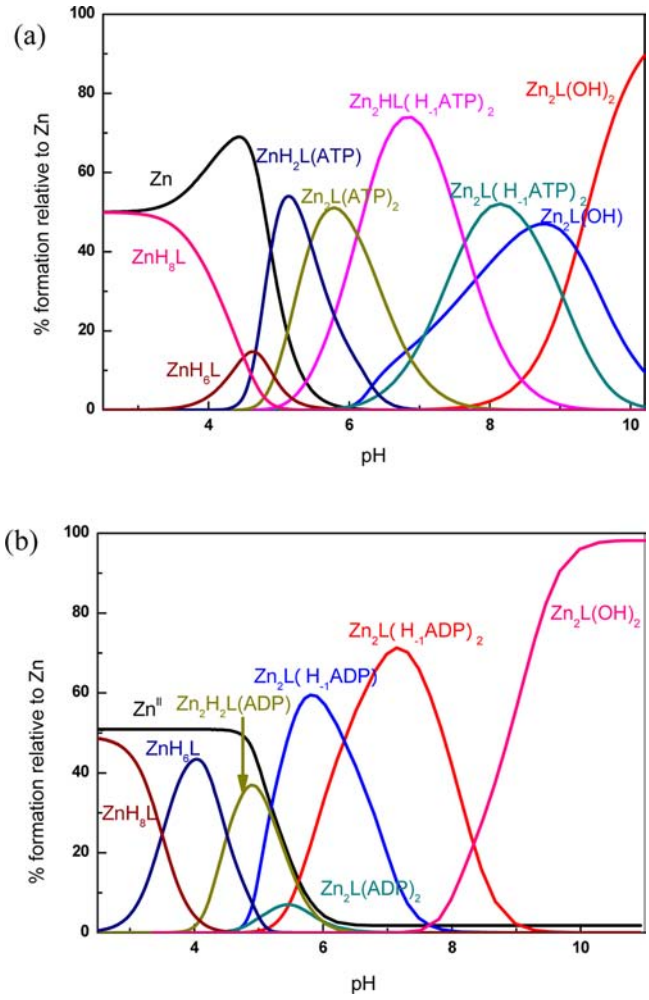

Figure 3. Distribution diagrams for the ternary systems Zn^{2+}–L–ATP (a) and Zn^{2+}–L–ADP (b) in aqueous solution as a function of pH. ([L] = 10^{-4} M, $[Zn^{2+}]$ = [ATP] = [ADP] = 2×10^{-4} M, 0.1 M NaCl, 298.1 K, charges are omitted).

system, the most stable species are $[Zn_2HL(H_{-1}ATP)_2]^-$ and $[Zn_2L(H_{-1}ATP)_2]^{2-}$ at pH 7.40, with the association constants (log K) of 11.49 (3.1×10^{11} M^{-1}) and 11.45 (2.8×10^{11} M^{-1}), respectively. For the ADP system, $[Zn_2L]^{4+}$ forms a more stable species of $[Zn_2L(H_{-1}ADP)_2]^{2-}$ at pH 7.40, with an association constant (log K) of 13.17 (1.5×10^{13} M^{-1}). The above results demonstrate that the main species are the 1:2 adducts of $[Zn_2L]^{4+}$ with ATP and ADP at physiological pH 7.40, and the larger association constant of $[Zn_2L(H_{-1}ADP)_2]^{2-}$ demonstrates that the interaction between $[Zn_2L]^{4+}$ and ADP is stronger than that between $[Zn_2L]^{4+}$ and ATP.

^{31}P NMR Spectral Studies. Though ATP, ADP, and AMP possess similar structures, they induce different fluorescence

dx.doi.org/10.1021/ic302435g | Inorg. Chem. 2013, 52, 4873–4879

changes of **1** (see Figure 2a). To investigate the binding characteristics of Zn(II) ions in **1** toward polyphosphate species in ATP, ADP, and AMP, ^{31}P NMR experiments were carried out (see Figure S7, Supporting Information). Upon addition of 0.5 equiv of **1** to ATP, the peaks corresponding to β- and γ-phosphate of ATP displayed significant downfield shifts, with $\Delta\delta$ values of 1.85 and 4.8 ppm for β- and γ-phosphates, respectively, while the peak corresponding to the α-phosphate showed a slight downfield shift ($\Delta\delta$ = 0.71 ppm). These data suggest that the two Zn(II) ions in **1** predominantly bind to β- and γ-phosphates rather than α-phosphate. As for ADP, the peaks of α- and β-phosphates of ADP shifted downfield significantly upon addition of 0.5 equiv of **1**, with $\Delta\delta$ values of 3.07 and 4.8 ppm, respectively, indicating that the two Zn(II) ions in **1** bind to α- and β-phosphates of ADP. The larger downfield shifts for ADP also demonstrate that the interaction between **1** and ADP is stronger than that between **1** and ATP. In contrast to the case for ATP and ADP, the chemical shift of α-phosphate in AMP scarcely changed upon addition of 0.5 equiv of **1** (Figure S7). The above results demonstrate that the Zn(II) ions in **1** can only bind to polyphosphate species in ATP and ADP via coordination interactions with both of the terminal phosphate groups and cannot bind to the monophosphate group in AMP.

Crystal Structure of 2·19H$_2$O. In order to better understand the binding mode of **1** with ATP and ADP, many attempts have been made to grow crystals of **1** with ATP and ADP, but these have all failed. However, single crystals of $[Zn_2L](P_2O_7)$ (**2**), which were prepared by the reaction of **1** with $Na_4P_2O_7\cdot 10H_2O$, were successfully obtained, and its structure was investigated. As shown in Figure 4, each Zn(II)

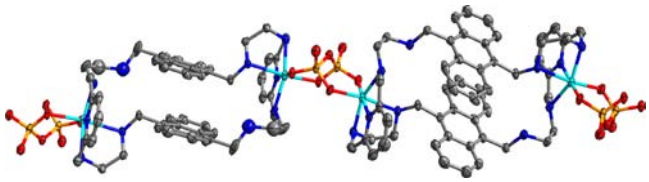

Figure 4. Thermal ellipsoid plot of the 1D chain of $[Zn_2L](P_2O_7)$ (**2**) with ellipsoids drawn at the 50% probability level.

ion in **2** displays a distorted-octahedral coordination geometry, by coordination with four nitrogen atoms from L in a folded configuration and two oxygen atoms from a pyrophosphate anion. In **2**, μ_2-pyrophosphate anions alternately link $[Zn_2L]^{4+}$ cations to generate a 1D coordination polymer. The result demonstrates that each Zn(II) ion from both sides of the macrocycle can coordinate with two phosphate groups from one pyrophosphate. The two anthracene rings in **2** are subparallel, with the shortest centroid−centroid distance being 3.85 Å. This distance is shorter than that of 3.95 Å in **1**, indicating that the two anthracene rings in **2** become closer and more parallel after the formation of **2**.

Binding Mode of 1 with ATP and ADP. To better understand the binding mode of $[Zn_2L]^{4+}$ with ATP and ADP, the structures of $[Zn_2L(ATP)_2]$ and $[Zn_2L(ADP)_2]$ were calculated by DFT calculations, and the calculated structures are shown in Figure 5. As shown in Figure 5, the coordination mode of Zn(II) in $[Zn_2L(ATP)_2]$ and $[Zn_2L(ADP)_2]$ is similar to that of Zn(II) in **2**, in which each Zn(II) ion is six-coordinated to four nitrogen atoms from L and two oxygen atoms from two terminal phosphate groups of ATP/ADP. Two

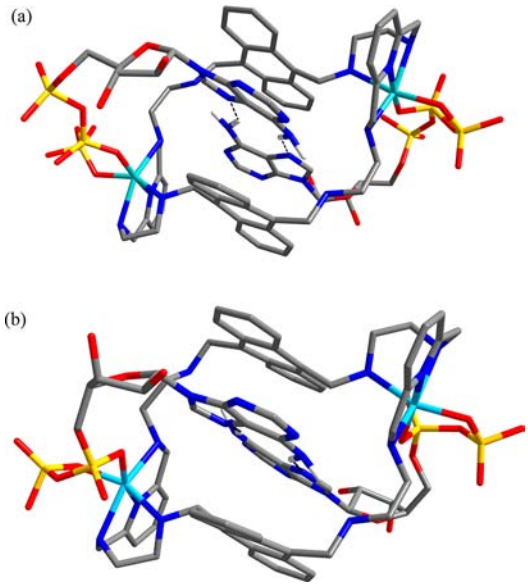

Figure 5. Calculated structures of $[Zn_2L]^{4+}$ with ATP (a) and ADP (b). The hydrogen bonds between two adenine groups are denoted as black dotted lines.

adenine groups from two ATP/ADP anions are base-paired via hydrogen bonding and insert into the two anthracene moieties of L through the $\pi\cdots\pi$ stacking of anthracene−adenine−anthracene to form a sandwichlike structure.[20] Two hydrogen-bonded adenine groups in $[Zn_2L(ADP)_2]$ are more coplanar than those in $[Zn_2L(ATP)_2]$ (Figure 5), as the dihedral angles of two base-paired adenine groups in $[Zn_2L(ADP)_2]$ and $[Zn_2L(ATP)_2]$ are 10.43 and 19.59°, respectively. Thus, the $\pi\cdots\pi$ stacking interactions of anthracene−adenine−anthracene in $[Zn_2L(ADP)_2]$ are stronger than those in $[Zn_2L(ATP)_2]$; the shortest centroid−centroid distances and dihedral angles between two adenine groups and two anthracene rings are 3.65 Å/8.09° and 3.83 Å/2.35° in $[Zn_2L(ADP)_2]$, while these values in $[Zn_2L(ATP)_2]$ are 3.81 Å/5.16° and 3.85 Å/11.55°. From the above results it can be found that the highly selective recognition of **1** toward adenosine polyphosphates can be attributed to its unique structure. First, **1** possesses recognition sites for both phosphate and adenine groups in ATP and ADP. Second, the sandwichlike binding mode between two anthracene moieties of L and a pair of adenine groups in ATP/ADP enhances the selectivity and affinity of **1** toward ATP/ADP. To the best of our knowledge, such a bridging bis-anthracene-type motif has not been observed in the reported chemosensors.

Biological Application of 1. Taking advantage of the selective sensing ability of **1** toward ATP and ADP, the biological application of **1** in cultured cells (HeLa cells) was investigated.[21] HeLa cells were grown in DMEM medium (Dulbecco's modified Eagle's medium) for 22 h. For comparison, one group of cells was treated with apyrase in PBS (pH 6.13) for 70 min, and another group was not treated. Then two groups of cells were exposed to 100 μM of **1** for 15 min at 37 °C and washed with PBS buffer solution (pH 7.40). It has been known that apyrase, a hydrolytic enzyme, can convert ATP or ADP into AMP and inorganic phosphate (Pi).[22] Microscopic observation was performed with a laser scanning confocal microscope (Zeiss LSM710). Images were recorded with a excitation wavelength of 405 nm. As shown in

dx.doi.org/10.1021/ic302435g | Inorg. Chem. 2013, 52, 4873−4879

Figure 6a, a bright blue fluorescence, with emission wavelengths of 440−480 nm, was observed inside the cells, while almost no

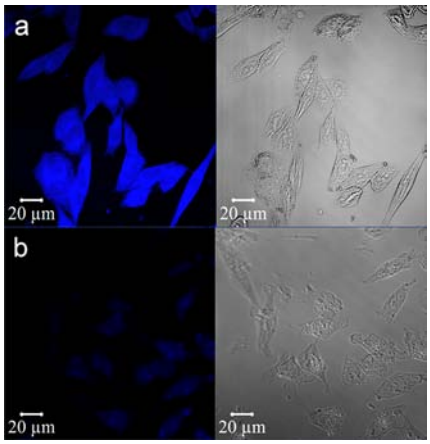

Figure 6. Fluorescence image (left) and optical image (right) of HeLa cells incubated with **1** (a) and images of another group of HeLa cells treated with apyrase and then incubated with **1** (b).

fluorescence was found in the other group of cells which were treated with apyrase (Figure 6b). These results suggest that **1** can allow the visualization of the ATP and ADP in living cells.

CONCLUSION

We have developed the novel fluorescent chemosensor **1**, which can effectively and selectively recognize ATP and ADP over other structurally similar nucleoside polyphosphates in aqueous solution at physiological pH 7.40. We demonstrated that the chemosensor **1** selectively recognizes adenosine polyphosphates on the basis of a unique binding mode. That is, the two Zn(II) ions in **1** can catch two ATP or ADP anions through coordination interactions between Zn(II) and the polyphosphate groups, and the two anthracene moieties in **1** can interact with adenine groups from two ATP or ADP anions through stacking interactions to form a sandwichlike structure; these multiple recognition interactions between **1** and ATP/ADP enhance the affinity and selectivity of **1** toward ATP/ADP, demonstrating that the selectivity can be enhanced through increasing the recognition sites of a chemosensor toward a certain nucleoside polyphosphate. Though μ_2-PPi anions can alternately link $[Zn_2L]^{4+}$ cations in **2** to generate a 1D coordination polymer of $\{[Zn_2L](P_2O_7)\}_n$, the results of competitive binding experiments of **1** with ATP/ADP in the presence of PPi demonstrate that the binding of **1** with ATP/ADP is almost completely unaffected by PPi anions, probably due to the stronger affinity of **1** toward ATP/ADP resulting from the multiple recognition interactions between **1** and ATP/ADP. In addition, **1** can be used for fluorescence imaging of adenosine polyphosphates in living cells. We believe that these novel findings are important for designing new chemosensors to increase the selectivity and binding ability for a certain nucleoside polyphosphate.

ASSOCIATED CONTENT

Supporting Information

Tables, figures, and CIF files giving association constants, Cartesian coordinates for the calculated structures, Job plots, fluorescence spectra, distribution diagrams, ^{31}P NMR spectra in DMSO-d_6, and X-ray crystallographic data for **1**·1.5H_2O·2CH_3CN and **2**·19H_2O. This material is available free of charge via the Internet at http://pubs.acs.org.

AUTHOR INFORMATION

Corresponding Author

*T.-B.L.: fax, +86-20-84112921; e-mail, lutongbu@mail.sysu.edu.cn.

Notes

The authors declare no competing financial interest.

ACKNOWLEDGMENTS

This work was supported by the 973 Program of China (2012CB821705), the NSFC (Grant Nos. 91127002, 21121061, and 20831005), and the NSF of Guangdong Province (S2012030006240).

REFERENCES

(1) (a) Pawson, T.; Scott, J. D. *Trends Biochem. Sci.* **2005**, *30*, 286−290. (b) Hargrove, A. E.; Nieto, S.; Zhang, T.; Sessler, J. L.; Anslyn, E. V. *Chem. Rev.* **2011**, *111*, 6603−6782. (c) Yaffe, M. B. *Nat. Rev. Mol. Cell Biol.* **2002**, *3*, 177−186. (d) Wang, D.; Zhang, X.; He, C.; Duan, C. *Org. Biomol. Chem.* **2010**, *8*, 2923−2925.

(2) (a) Knowles, J. R. *Annu. Rev. Biochem.* **1980**, *49*, 877−919. (b) Gourine, A. V.; Llaudet, E.; Dale, N.; Spyer, K. M. *Nature* **2005**, *436*, 108−111. (c) Wu, H.; He, C.; Lin, Z.; Liu, Y.; Duan, C. *Inorg. Chem.* **2009**, *48*, 408−410.

(3) (a) Berg, J.; Hung, Y. P.; Yellen, G. *Nat. Methods* **2009**, *6*, 161−166. (b) Lu, L.; Zhang, X.; Kong, R.; Yang, B.; Tan, W. *J. Am. Chem. Soc.* **2011**, *133*, 11686−11691.

(4) (a) Nakano, S.; Mashima, T.; Matsugami, A.; Inoue, M.; Katahira, M.; Morii, T. *J. Am. Chem. Soc.* **2011**, *133*, 4567−4579. (b) Descalzo, A. B.; Marcos, M. D.; Martinez-Manez, R.; Soto, J.; Beltran, D.; Amoros, P. *J. Mater. Chem.* **2005**, *15*, 2721−2731. (c) McCleskey, S. C.; Griffin, M. J.; Schneider, S. E.; McDevitt, J. T.; Anslyn, E. V. *J. Am. Chem. Soc.* **2003**, *125*, 1114−1115. (d) Li, C.; Numata, M.; Takeuchi, M.; Shinkai, S. *Angew. Chem., Int. Ed.* **2005**, *44*, 6371−6374. (e) Schneider, S. E.; O'Neil, S. N.; Anslyn, E. V. *J. Am. Chem. Soc.* **2000**, *122*, 542−543. (f) Zyryanov, J. V.; Palacios, M. A.; Anzenbacher, P. *Angew. Chem., Int. Ed.* **2007**, *46*, 7849−7852.

(5) (a) Wang, S.; Chang, Y. T. *J. Am. Chem. Soc.* **2006**, *128*, 10380−10381. (b) Chen, X.; Jou, M. J.; Yoon, J. *Org. Lett.* **2009**, *11*, 2181−2184. (c) Kim, H. N.; Moon, J. H.; Kim, S. K.; Kwon, J. Y.; Jang, Y. J.; Lee, J. Y.; Yoon, J. *J. Org. Chem.* **2011**, *76*, 3805−3811.

(6) (a) Jose, D. A.; Mishra, S.; Ghosh, A.; Shrivastav, A.; Mishra, S. K.; Das, A. *Org. Lett.* **2007**, *9*, 1979−1982. (b) Kejik, Z.; Zaruba, K.; Michalik, D.; Sebek, J.; Dian, J.; Pataridis, S.; Volka, K.; Kral, V. *Chem. Commun.* **2006**, *14*, 1533−1535. (c) Ambrosi, G.; Formica, M.; Fusi, V.; Giorgi, L.; Guerri, A.; Macesi, E.; Micheloni, M.; Paosi, P.; Pontellini, R.; Rossi, P. *Inorg. Chem.* **2009**, *48*, 5901−5912. (d) Khatua, S.; Choi, S. H.; Lee, J.; Kim, K.; Do, Y.; Churchill, D. G. *Inorg. Chem.* **2009**, *48*, 2993−2999. (e) Kim, K.; Ha, Y.; Kaufman, L.; Churchill, D. G. *Inorg. Chem.* **2012**, *51*, 928−938.

(7) (a) Ojida, A.; Nonaka, H.; Miyahara, Y.; Tamaru, S.; Sada, K.; Hamachi, I. *Angew. Chem., Int. Ed.* **2006**, *45*, 5518−5521. (b) Ojida, A.; Miyahara, Y.; Wongkongkatep, J.; Tamaru, S.; Sada, K.; Hamachi, I. *Chem. Asian J.* **2006**, *1*, 555−563. (c) Ojida, A.; Takashima, I.; Kohira, T.; Nonaka, H.; Hamachi, I. *J. Am. Chem. Soc.* **2008**, *130*, 12095−12101. (d) Kurishita, Y.; Kohira, T.; Ojida, A.; Hamachi, I. *J. Am. Chem. Soc.* **2010**, *132*, 13290−13299. (e) Kurishita, Y.; Kohira, T.; Ojida, A.; Hamachi, I. *J. Am. Chem. Soc.* **2012**, *134*, 18779−18789.

(8) (a) Xu, Z. C.; Singh, N. J.; Lim, J.; Pan, J.; Kim, H.; Park, S.; Kim, K. S.; Yoon, J. *J. Am. Chem. Soc.* **2009**, *131*, 15528−15533. (b) Neelakandan, P. P.; Hariharan, M.; Ramaiah, D. *J. Am. Chem. Soc.* **2006**, *128*, 11334−11335. (c) Kwon, J. Y.; Singh, N. J.; Kim, H.; Kim, S. K.; Kim, K. S.; Yoon, J. *J. Am. Chem. Soc.* **2004**, *126*, 8892−8893. (d) Bazzicalupi, C.; Biagini, S.; Bencini, A.; Faggi, E.; Giorgi, C.;

Matera, I.; Valtancoli, B. *Chem. Commun.* **2006**, 4087−4089. (e) Kaur, J.; Singh, P. *Chem. Commun.* **2011**, *47*, 4472−4474.
(9) Rao, A. S.; Kim, D.; Nam, H.; Jo, H.; Kim, K. H.; Ban, C.; Ahn, K. H. *Chem. Commun.* **2012**, *48*, 3206−3208.
(10) Chen, Z. H.; Zhou, F. G.; Zhang, Y. Q.; Zhu, Q. J.; Xue, S. F.; Tao, Z. *J. Mol. Struct. (THEOCHEM)* **2009**, *930*, 140−146.
(11) Koz, G.; Özdemir, N.; Astley, D.; Dinçer, M.; Astley, S. T. *J. Mol. Struct. (THEOCHEM)* **2010**, *966*, 39−47.
(12) Churchill, D. G. *J. Chem. Educ.* **2006**, *83*, 1798−1803.
(13) Bag, B.; Bharadwaj, P. K. *J. Phys. Chem. B* **2005**, *109*, 4377−4390.
(14) Gran, G. *Acta Chem. Scand.* **1950**, *4*, 559.
(15) Gran, P.; Sabatini, A.; Vacca, A. *Hyperquad 2000*; University of Leeds, Leeds, U.K., 2000.
(16) Sheldrick, G. M. *SHELXS 97, Program for Crystal Structure Refinement*; University of Göttingen, Göttingen, Germany, 1997.
(17) *Accelrys, Materials Studio Getting Started, release 5.0*; Accelrys Software, Inc., San Diego, CA, 2009.
(18) Kim, M. J.; Swamy, K. M. K.; Lee, K. M.; Jagdale, A. R.; Kim, Y.; Kim, S.; Yoo, K. H.; Yoon, J. *Chem. Commun.* **2009**, 7215−7217.
(19) Sclafani, J. A.; Maranto, M. T.; Sick, T. M.; Van Arman, S. A. *Tetrahedron Lett.* **1996**, *37*, 2193−2196.
(20) Neelakandan, P. P.; Hariharan, M.; Ramaiah, D. *Org. Lett.* **2005**, *7*, 5765−5768.
(21) Yagutkin, G. G.; Mikhailov, A.; Samburski, S. S.; Jalkanen, S. *Mol. Biol. Cell* **2006**, *17*, 3378−3385.
(22) Zimmermann, H. *Trends Pharmacol. Sci.* **1999**, *20*, 231−236.

dx.doi.org/10.1021/ic302435g | *Inorg. Chem.* 2013, 52, 4873−4879